AIAA JOURNAL
Vol. 45, No. 10, October 2007

Optimization of Long Anisotropic Laminated Fiber Composite Panels with T-Shaped Stiffeners

J. Enrique Herencia,* Paul M. Weaver,† and Michael I. Friswell‡
University of Bristol, Bristol, BS8 1TR England, United Kingdom

DOI: 10.2514/1.26321

A method to optimize long anisotropic laminated fiber composite panels with T-shaped stiffeners is presented. The technique splits the optimization problem into two steps. At the first step, composite optimization is performed using mathematical programming in which the skin and the stiffeners are characterized by lamination parameters accounting for their membrane and flexural anisotropy. Skin and stiffener laminates are assumed to be symmetric or midplane symmetric laminates with 0-, 90-, 45-, or −45- deg ply angles. The stiffened panel consists of a series of skin-stiffener assemblies or superstiffeners. Each superstiffener is further idealized as a group of flat laminated plates that are rigidly connected. The stiffened panel is subjected to a combined loading under strength, buckling, and practical-design constraints. At the second step, the actual skin and stiffener layups are obtained using a genetic algorithm and considering the ease of manufacture. This approach offers the advantage of introducing numerical analysis methods such as the finite element method at the first step, without significant increases in processing time. Furthermore, modeling the laminate anisotropy enables the designer to explore and potentially use elastic tailoring in a beneficial manner.

Nomenclature

A	=	membrane stiffness matrix, membrane
A_{ij}	=	terms of the membrane stiffness matrix, $i = j = 1, 2, 6$
A_{sf}	=	area of the stiffener flange
A_{skin}	=	area of the skin
A_{stg}	=	area of the stiffener
A_{sw}	=	area of the stiffener web
a	=	panel length
B	=	membrane-bending coupling stiffness matrix
b	=	panel width
b_{sf}	=	stiffener flange width
C	=	compression
c	=	continuous
D	=	bending stiffness matrix
D_c	=	bending stiffness of the superstiffener element per unit width
D_{ij}	=	terms of the bending stiffness matrix, $i = j = 1, 2, 6$
d	=	discrete
E_{ij}	=	Young's modulus in the ij direction, $i = j = 1, 2$
EI_c	=	longitudinal bending stiffness of the superstiffener element
F_c	=	longitudinal force applied at the superstiffener centroid
G_i	=	ith design constraint
G_{ij}	=	shear modulus, $i = 1$ and $j = 2$
G_{xy}^{sw}	=	shear modulus of the stiffener web
h	=	laminate thickness
h_{sw}	=	stiffener web height
K_i	=	buckling coefficient, $i = x, xy$, sh
M	=	mass of the superstiffener element, running-moment vector
MS	=	midplane symmetric
M_i	=	mass, $i = c, d$
N	=	running load vector
N_i	=	load per unit length in the i direction, $i = x, y, xy$
N_i^{cr}	=	critical load per unit length, $i = x, xy, wx$, sh
n_c	=	number of design constraints
n_v	=	number of design variables
P_{cr}	=	critical buckling load of a column accounting for transverse shear loading
P_e	=	Euler buckling load
p	=	maximum number of plies of the same orientation that can be stacked together
Q_{ij}	=	terms of the reduced stiffness matrix, $i = j = 1, 2, 6$
RF_i^j	=	reserve factor, $i = px, pxy$, pb, wb, cb, sb, cs, T, C, b and $j = x, y, xy$
S	=	symmetric
skin	=	skin
stg	=	stiffener
sf	=	stiffener flange
sw	=	stiffener web
t	=	thickness of the skin
t_a	=	thickness of the stiffener flange
t_{sf}	=	total thickness of the stiffener flange
t_{sw}	=	thickness of the stiffener web
t_w	=	thickness of the web
T	=	tension
U_i	=	material invariants, $i = 1 \ldots 5$
wf_i^j	=	weighting factor for lamination parameters, $i = 1, 2, 3$; $j = A, D$
$\boldsymbol{x}, x$	=	vector of design variables, abscise
$\boldsymbol{y}, y$	=	gene, ordinate
$\alpha, \beta, \gamma, \delta$	=	nondimensional parameters
ε_i^{0j}	=	laminate applied strain, $i = T, C$; $j = x, y, xy$
$\varepsilon_{\mathrm{ai}}^j$	=	laminate allowable strain, $i = T, C$; $j = x, y, xy$
ζ	=	tolerance value
κ	=	middle surface curvatures
λ_i	=	buckling or strength load factor (eigenvalue), $i = b, s$

Presented as Paper 2171 at the 47th AIAA/ASME/ASCE/AHS/ASC Structures, Structural Dynamics and Materials Conference, Newport, RI, 1–4 May 2006; received 4 July 2006; revision received 6 April 2007; accepted for publication 17 April 2007.

*Marie Curie Research Assistant, Department of Aerospace Engineering, Queen's Building. Student Member AIAA.

†Reader, Department of Aerospace Engineering, Queen's Building. Member AIAA.

‡Sir George White Professor of Aerospace Engineering, Department of Aerospace Engineering, Queen's Building. Member AIAA.

ν_i = Poisson's ratio in the i direction, $i = 12, 21$
ξ_i^j = lamination parameters, $i = 1, 2, 3$; $j = A, D$
ρ = density
φ = fiber-orientation angle
θ, ψ, ϕ = encoded ply angle for the skin, stiffener flange, and web, respectively

I. Introduction

THE use of composite materials as primary structures in the commercial aviation industry has been gradually increasing over the last decade. This has culminated in programs such as the Airbus A350 or the Boeing 787, for which composite materials will play a major role. Primary flight composite structures such as wings or fuselages are mainly designed using stiffened panels. In general, composite materials present high specific strength and stiffness ratios [1]. Furthermore, structures made of composite materials can be stiffness-tailored, potentially offering a significant advantage over their metallic counterparts. This latter feature is intimately related to their design and manufacture. Because of practical, yet often limiting, manufacturing considerations, laminated fiber composite panels have been restricted to symmetric or midplane symmetric laminates with 0-, 90-, 45-, or −45- deg ply angles. The manufacture of the T-shaped stiffeners adds an additional degree of complexity, because it allows the modification of the stiffener web and flange by adding extra plies and capping plies, respectively. This paper is inspired by the desire to design elastically tailored composite stiffened panels while considering manufacturing requirements commonly used in the aerospace industry.

Over the years, optimization techniques have been developed to assist engineers with composite design [2–34]. The nature of composite optimization is nonlinear. In the seventies, early attempts for the optimization of laminated fiber composites were performed by Schmit and Farshi [2,3]. They optimized symmetric laminated fiber composite materials having homogeneous and orthotropic properties, considering the ply thicknesses as continuous variables. They transformed the nonlinear problem into a sequence of linear problems. In the same light, Stroud and Agranoff [4] optimized composite hat-stiffened and corrugated panels using nonlinear mathematical techniques with a simplified set of buckling equations as constraints. The width and thickness of the elements of the dimensioned cross section were the design variables. They assumed that the laminates were orthotropic. However, although designed carefully, composites might exhibit some degree of flexural anisotropy. Ashton and Waddoups [5] initially showed the effect of the flexural anisotropy on the stability of composite plates. Chamis [6] concluded that neglecting flexural anisotropy in the evaluation of buckling behavior could lead to nonconservative results. Later, Nemeth [7] characterized the importance of flexural anisotropy and provided bounds within which its effect would be significant. Recently, Weaver [8] developed closed-form (CF) solutions to quantify the effect of flexural anisotropy on compression loads. Flexural anisotropy is intrinsically related to the laminate stacking sequence. The addressing of the laminate stacking sequence, and hence the identification of the number of plies of each fiber orientation, converts the layup optimization problem into a nonlinear problem with discrete variables that has a nonconvex design space.

Tsai et al. [9] and Tsai and Hahn [10] gave an alternative representation of the stiffness properties of a laminated fiber composite panel by introducing lamination parameters. Miki and Sugiyama [11] proposed the use of lamination parameters to deal with the discrete laminate stacking-sequence problem; they assumed symmetric and orthotropic laminates. Optimum designs for the required in-plane stiffness, buckling strength, and so on were obtained from geometric relations between the lamination-parameter feasible region and the objective function. Fukunaga and Vanderplaats [12] used lamination parameters and mathematical programming (MP) techniques to perform stiffness optimization of orthotropic laminated composites. Cylindrical shells under combined loading were used as a practical application. Haftka and Walsh [13] used integer programming techniques to carry out laminate stacking-sequence optimization under buckling constraints on symmetric and balanced laminated plates. They used zero–one integers as design variables that were related to stiffness properties via lamination parameters and showed that the problem was linear. Flexural anisotropy was limited to manually modifying the optimum design and they used the branch-and-bound method to solve the problem. Nagendra et al. [14] extended the previous work and optimized the stacking sequence of symmetric and balanced composite laminates with stability and strain constraints. Unfortunately, integer programming techniques require large computational resources, especially when structure complexity increases. Fukunaga et al. [15] presented an approach to maximize buckling loads under combined loading of symmetrically laminated plates, including the bending–twisting couplings or flexural anisotropy. They employed MP techniques and the lamination parameters as design variables. They confirmed the detrimental effect of the flexural anisotropy on the buckling load of panels under normal loading and highlighted that under shear and shear-normal loading, flexural anisotropy could increase or decrease the critical buckling load. Although an optimal laminate stacking sequence with optimal fiber orientation was presented, neither discrete nor practical laminates were shown.

A different strategy was adopted by Le Riche and Haftka [16] and later by Nagendra et al. [17,18]. They employed genetic algorithms (GAs) to solve the integer stacking-sequence problem. GAs are search algorithms based on the mechanics of natural selection and natural genetics [19], which do not require gradient information to perform the search. GAs are widely used for their ability to tackle search spaces with many local optima [20] and, therefore, a nonconvex design space. Nagendra et al. [17] also investigated the application of a GA to the design of blade-stiffened composite panels. VIPASA [21] was used as the analysis tool and results were compared with PASCO [22], which uses VIPASA as the analysis tool and CONMIN [23] as the optimizer. It was concluded that the designs obtained by the GA offered higher performance than the continuous designs. However, it was recognized that great computational cost was associated with the GA. Earlier, Bushnell [24] used PANDA2 [25] to find the minimum weight design of composite flat and curved stiffened panels. Local and global buckling loads were calculated by either CF expressions or discretized models of the panel cross sections. It was shown that PANDA2 could have structure dimensions, thicknesses, and ply angles as design variables. Results were compared with the literature and with STAGS [26]. More recently, Liu et al. [27] employed VICONOPT [28] to perform an optimization of composite stiffened panels under strength, buckling, and practical-design constraints; a bilevel approach was adopted. VICONOPT was employed at the first level to minimize the panel weight, employing equivalent orthotropic properties for the laminates with continuous thicknesses, whereas at the second level, laminate thicknesses were rounded up and associated to predetermined design layups.

A two-level optimization strategy combining lamination parameters MP and GAs was initially proposed by Yamazaki [29]. The optimization was split into two parts. First, a gradient-based optimization was performed using the in-plane and out-of-plane lamination parameters as design variables. Second, the lamination parameters from the first level were targeted using a GA. In this paper, the volume, buckling load, deflection, and natural frequencies of a composite panel were optimized without accounting for either membrane or flexural anisotropy. Autio [30], following a similar approach, investigated actual layups. The approach adopted was similar to Yamazaki's [29], the difference being that commercial uni/multiaxial plies were considered and certain layup design rules were introduced as penalties in the fitness function of the GA code. Earlier, Todoroki and Haftka [31] proposed a more sophisticated approach; they divided the optimization into two stages. First, the lamination parameters were used in a continuous optimization to identify the neighborhood of the optimum design. Subsequently, a response surface approximation was created in that neighborhood and the GA was applied to that approximation. They applied this procedure to buckling load maximization of a composite plate. However, with the

exception of Fukunaga and Vanderplats [12], none of the previous authors considered the feasible region in the lamination parameter space that relates in-plane, coupling, and out-of-plane lamination parameters.

Liu et al. [32] employed lamination parameters and defined the feasible region between two of the four membrane and bending lamination parameters to maximize the buckling load of unstiffened composite panels with restricted ply angles. They compared their approach against one using a GA and concluded that the use of lamination parameters in a continuous optimization produced similar results to those obtained by the GA, except in cases in which laminates were thin or had low aspect ratios. Furthermore, Liu and Haftka [33] proposed a single-level weight minimization of composite wing structures using flexural lamination parameters. They assumed continuous thicknesses for a set of restricted ply angles and two flexural lamination parameters as design variables. Their constraints were strength, buckling, and the flexural lamination-parameters domain. The wing consisted of several unstiffened composite panels with orthotropic properties. They compared their work against a two-level wing optimization strategy using GAs and concluded that both approaches produced similar results and that the single level approach provided a lower bound to the true optima.

Diaconu and Sekine [34] performed layup optimization of laminated composite shells for maximization of the buckling load using the lamination parameters as design variables and including their feasible region. They fully defined, for the first time, the relations between the membrane, coupling, and bending lamination parameters for ply angles restricted to 0, 90, 45, and −45 deg, to identify their feasible region within the design space. Note that although developed independently of each other, their definition of the feasible region for the lamination parameters was consistent with that provided by Liu et al. [32] (only defined for two membrane and bending lamination parameters with ply angles restricted to 0, 90, 45, and −45 deg).

The aim of the present paper is to provide an approach to optimize long anisotropic laminated fiber composite panels with T-shaped stiffeners. The technique splits the optimization problem into two steps. At the first step, composite optimization is performed using MP, in which the skin and the stiffeners are characterized by lamination parameters accounting for their membrane and flexural anisotropy. The skin and stiffener laminates are assumed to be symmetric or midplane symmetric laminates with 0-, 90-, 45-, or −45- deg ply angles. The stiffened panel consists of a series of skin-stiffener assemblies or superstiffeners. Each superstiffener is further idealized as a group of the flat laminated plates rigidly connected. The stiffened panel is subjected to a combined loading under strength, buckling, and practical-design constraints. At the second step, the actual skin and stiffener layups are obtained using a GA and considering the ease of manufacture. This approach offers the advantage of introducing numerical analysis methods such as the finite element (FE) method at the first step, without significant increases in processing time. Furthermore, modeling the laminate anisotropy enables the designer to explore and potentially use elastic tailoring in a beneficial manner. The novelty of the current approach is based upon the inclusion of membrane and flexural anisotropy for elastic tailoring purposes, manufacturing details of the stiffener, practical-design constraints on layups, and the interaction between membrane and flexural lamination parameters for stiffened panels.

II. Stiffened-Panel Geometry and Loading

The composite stiffened panel is assumed to be wide and composed of a series of skin-stiffener assemblies or superstiffeners, as shown in Fig. 1. Each superstiffener consists of three flat plates that are considered to be rigidly connected (all degrees of freedom match at the interface), corresponding to the skin, stiffener flange, and stiffener web, respectively. The behavior of the stiffened panel can be modeled by a single superstiffener. Figure 2 defines the superstiffener geometry, material axis, and positive sign convention for the loading.

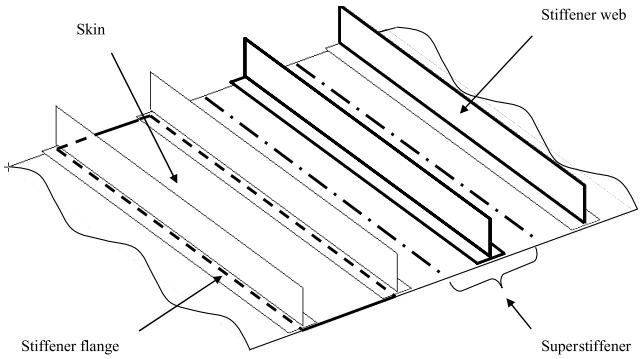

Fig. 1 Stiffened-panel elements.

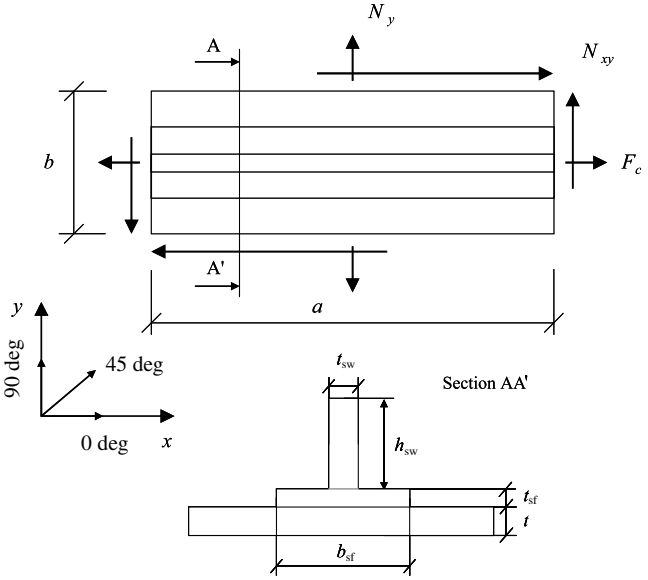

Fig. 2 Superstiffener element.

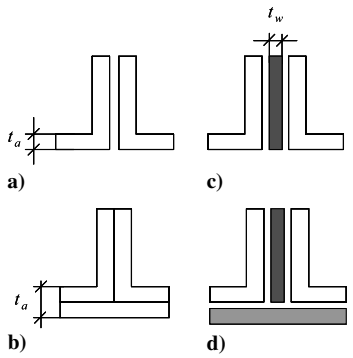

Fig. 3 T-shaped stiffener types.

The geometry of the stiffener is affected by its design and manufacturing process. For this study, four different stiffener configurations are considered. The stiffener is manufactured as a back-to-back angle (Fig. 3a), adding capping plies in the stiffener flange (Fig. 3b) or adding extra plies in the stiffener web (Fig. 3c) and a combination of the previous configurations (Fig. 3d).

III. Laminate Constitutive Equations

Laminate constitutive equations for the skin, stiffener flange, and stiffener web, respectively, are obtained by applying the classical laminate theory (CLT) [1] to each of them; thus,

$$\begin{bmatrix} N \\ M \end{bmatrix} = \begin{bmatrix} A & B \\ B & D \end{bmatrix} \begin{bmatrix} \varepsilon^0 \\ \kappa \end{bmatrix} \tag{1}$$

The preceding properties can be expressed in terms of material stiffness invariants U and 12 lamination parameters ξ [9,10]. Because laminates are considered to be symmetric or midplane symmetric, the membrane-bending coupling matrix B will vanish. This also reduces the number of lamination parameters to eight. In addition, individual plies are assumed to be orthotropic and laminated with only 0-, 90-, 45-, or −45- deg fiber angles; as a result, the lamination parameters are further decreased to six. The expressions for the membrane and bending stiffness terms are

$$\begin{bmatrix} A_{11} \\ A_{12} \\ A_{22} \\ A_{66} \\ A_{16} \\ A_{26} \end{bmatrix} = h \begin{bmatrix} 1 & \xi_1^A & \xi_2^A & 0 & 0 \\ 0 & 0 & -\xi_2^A & 1 & 0 \\ 1 & -\xi_1^A & \xi_2^A & 0 & 0 \\ 0 & 0 & -\xi_2^A & 0 & 1 \\ 0 & \frac{\xi_3^A}{2} & 0 & 0 & 0 \\ 0 & \frac{\xi_3^A}{2} & 0 & 0 & 0 \end{bmatrix} \begin{bmatrix} U_1 \\ U_2 \\ U_3 \\ U_4 \\ U_5 \end{bmatrix} \tag{2}$$

$$\begin{bmatrix} D_{11} \\ D_{12} \\ D_{22} \\ D_{66} \\ D_{16} \\ D_{26} \end{bmatrix} = \frac{h^3}{12} \begin{bmatrix} 1 & \xi_1^D & \xi_2^D & 0 & 0 \\ 0 & 0 & -\xi_2^D & 1 & 0 \\ 1 & -\xi_1^D & \xi_2^D & 0 & 0 \\ 0 & 0 & -\xi_2^D & 0 & 1 \\ 0 & \frac{\xi_3^D}{2} & 0 & 0 & 0 \\ 0 & \frac{\xi_3^D}{2} & 0 & 0 & 0 \end{bmatrix} \begin{bmatrix} U_1 \\ U_2 \\ U_3 \\ U_4 \\ U_5 \end{bmatrix} \tag{3}$$

The material stiffness invariants U are given as follows:

$$\begin{bmatrix} U_1 \\ U_2 \\ U_3 \\ U_4 \\ U_5 \end{bmatrix} = \frac{1}{8} \begin{bmatrix} 3 & 2 & 3 & 4 \\ 4 & 0 & -4 & 0 \\ 1 & -2 & 1 & -4 \\ 1 & -6 & 1 & -4 \\ 1 & -2 & 1 & 4 \end{bmatrix} \begin{bmatrix} Q_{11} \\ Q_{12} \\ Q_{22} \\ Q_{66} \end{bmatrix} \tag{4}$$

The lamina stiffness properties Q are related to the ply Young's moduli and Poisson's ratios by the following equations:

$$Q_{11} = \frac{E_{11}}{1 - \nu_{12}\nu_{21}} \tag{5}$$

$$Q_{12} = \frac{\nu_{12}E_{22}}{1 - \nu_{12}\nu_{21}} \tag{6}$$

$$Q_{22} = \frac{E_{22}}{1 - \nu_{12}\nu_{21}} \tag{7}$$

$$Q_{21} = Q_{12} \tag{8}$$

$$Q_{66} = G_{12} \tag{9}$$

$$\nu_{21} = \nu_{12}\frac{E_{22}}{E_{11}} \tag{10}$$

The membrane and bending lamination parameters are calculated, respectively, by the following integrals:

$$\xi^A_{[1\ 2\ 3]} = \frac{1}{h}\int_{-h/2}^{h/2} [\cos 2\varphi \quad \cos 4\varphi \quad \sin 2\varphi]\, \mathrm{d}z \tag{11}$$

$$\xi^D_{[1\ 2\ 3]} = \frac{12}{h^3}\int_{-h/2}^{h/2} [\cos 2\varphi \quad \cos 4\varphi \quad \sin 2\varphi] z^2\, \mathrm{d}z \tag{12}$$

IV. Optimization Strategy

The optimization strategy is shown in Fig. 4; it is divided into two steps. At the first step, the superstiffener is optimized using lamination parameters and gradient-based techniques. The dimensions and values of the lamination parameters for an optimum superstiffener design are obtained. At the second step, a GA is used to target the optimum lamination parameters to obtain the actual and manufacturable stacking sequences for the superstiffener laminates (skin, stiffener flange, and stiffener web).

A. First Step: Gradient-Based Optimization

At this step, a nonlinear constrained optimization is performed. The basic mathematical optimization problem can be expressed as follows:

Minimize:

$$M(\boldsymbol{x}) \tag{13}$$

Subject to:

$$G_i(\boldsymbol{x}) \le 0 \qquad i = 1, \ldots, n_c \tag{14}$$

$$x_j^l \le x_j \le x_j^u \qquad j = 1, \ldots, n_v \tag{15}$$

with

$$\boldsymbol{x} = \{x_1, x_2, \ldots, x_n\} \tag{16}$$

In this case, the objective function is the mass of the superstiffener element, and the inequality constraints are strength, local and global buckling, and practical-design requirements. The design variables are the thicknesses of the skin, stiffener flange and web, and their related membrane and bending lamination parameters, depending on the stiffener type. The side constraints are the bounds of those design variables. MATLAB [35] is employed to conduct the gradient-based optimization.

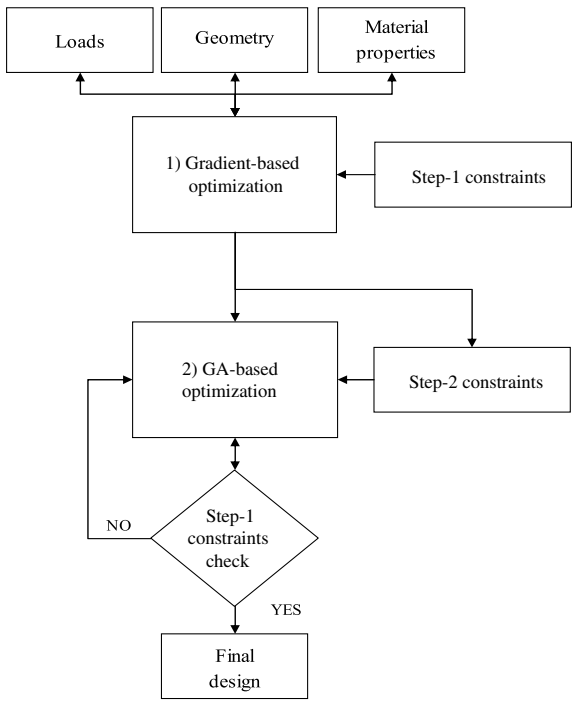

Fig. 4 Optimization flowchart.

1. Objective Function

The objective function is the mass of the superstiffener element. The mass as a function of the design variables, materials properties, and geometry is given by

$$M(\boldsymbol{x}) = a[\rho_{\text{skin}} A_{\text{skin}}(\boldsymbol{x}) + \rho_{\text{stg}} A_{\text{stg}}(\boldsymbol{x})] \tag{17}$$

where the skin and stiffener areas are defined as follows:

$$A_{\text{skin}} = t \cdot b \tag{18}$$

$$A_{\text{stg}} = A_{\text{sf}} + A_{\text{sw}} = t_{\text{sf}} \cdot b_{\text{sf}} + t_{\text{sw}} \cdot h_{\text{sw}} \tag{19}$$

2. Design Variables and Constraints

The design variables for the superstiffener element, depending on the stiffener type, are listed in Table 1. For stiffener types a, c, and d, sublaminates are employed to calculate the membrane and bending stiffness properties for the stiffener's web (stiffener types a, c, and d) and flange (stiffener type d), respectively.

Note that the stiffener web laminate is not the same as the web laminate. The stiffener web laminate is made of two stiffener flange laminates for stiffener type a, is equivalent to the stiffener flange laminate for stiffener type b, and is composed of three sublaminates (two outer stiffener flange laminates and one inner web laminate) for stiffener types c and d.

Four sets of design constraints are considered in the optimization of the superstiffener element. The following sections describe those constraints in detail.

3. Lamination-Parameter Constraints

It is shown (e.g., [11]) that the lamination parameters in either membrane, coupling, or bending must be bound. For a symmetric or midplane symmetric laminate with ply angles limited to 0, 90, 45 and −45 deg, the expressions for the membrane and bending lamination-parameter constraints are given by [11,34]

$$2|\xi_1^{A,D}| + \xi_2^{A,D} - 1 \le 0 \tag{20}$$

$$2|\xi_3^{A,D}| + \xi_2^{A,D} - 1 \le 0 \tag{21}$$

Additional constraints between the membrane, coupling, and bending lamination parameters were introduced by Diaconu and Sekine [34]. Their aim was to define the feasible region in the lamination-parameter design space with special consideration given to the compatibility between the membrane, coupling, and bending lamination parameters. Because there is a dependency between the membrane, coupling, and bending properties, it is this compatibility that enables the production of laminate designs that possess consistent properties. Accounting for symmetric laminates and rearranging terms, those expressions are

$$\left(\xi_i^A - 1\right)^4 - 4\left(\xi_i^D - 1\right)\left(\xi_i^A - 1\right) \le 0 \qquad i = 1,2,3 \tag{22}$$

$$\left(\xi_i^A + 1\right)^4 - 4\left(\xi_i^D + 1\right)\left(\xi_i^A + 1\right) \le 0 \qquad i = 1,2,3 \tag{23}$$

$$\left(2\xi_1^A - \xi_2^A - 1\right)^4 - 16\left(2\xi_1^D - \xi_2^D - 1\right)\left(2\xi_1^A - \xi_2^A - 1\right) \le 0 \tag{24}$$

$$\left(2\xi_1^A + \xi_2^A + 1\right)^4 - 16\left(2\xi_1^D + \xi_2^D + 1\right)\left(2\xi_1^A + \xi_2^A + 1\right) \le 0 \tag{25}$$

$$\left(2\xi_1^A - \xi_2^A + 3\right)^4 - 16\left(2\xi_1^D - \xi_2^D + 3\right)\left(2\xi_1^A - \xi_2^A + 3\right) \le 0 \tag{26}$$

$$\left(2\xi_1^A + \xi_2^A - 3\right)^4 - 16\left(2\xi_1^D + \xi_2^D - 3\right)\left(2\xi_1^A + \xi_2^A - 3\right) \le 0 \tag{27}$$

$$\left(2\xi_3^A - \xi_2^A + 1\right)^4 - 16\left(2\xi_3^D - \xi_2^D + 1\right)\left(2\xi_3^A - \xi_2^A + 1\right) \le 0 \tag{28}$$

$$\left(2\xi_3^A + \xi_2^A - 1\right)^4 - 16\left(2\xi_3^D + \xi_2^D - 1\right)\left(2\xi_3^A + \xi_2^A - 1\right) \le 0 \tag{29}$$

$$\left(2\xi_3^A - \xi_2^A - 3\right)^4 - 16\left(2\xi_3^D - \xi_2^D - 3\right)\left(2\xi_3^A - \xi_2^A - 3\right) \le 0 \tag{30}$$

$$\left(2\xi_3^A + \xi_2^A + 3\right)^4 - 16\left(2\xi_3^D + \xi_2^D + 3\right)\left(2\xi_3^A + \xi_2^A + 3\right) \le 0 \tag{31}$$

$$\left(\xi_1^A - \xi_3^A - 1\right)^4 - 4\left(\xi_1^D - \xi_3^D - 1\right)\left(\xi_1^A - \xi_3^A - 1\right) \le 0 \tag{32}$$

$$\left(\xi_1^A + \xi_3^A + 1\right)^4 - 4\left(\xi_1^D + \xi_3^D + 1\right)(\xi_1^A + \xi_3^A + 1) \le 0 \tag{33}$$

$$\left(\xi_1^A - \xi_3^A + 1\right)^4 - 4\left(\xi_1^D - \xi_3^D + 1\right)\left(\xi_1^A - \xi_3^A + 1\right) \le 0 \tag{34}$$

$$\left(\xi_1^A + \xi_3^A - 1\right)^4 - 4\left(\xi_1^D + \xi_3^D - 1\right)\left(\xi_1^A + \xi_3^A - 1\right) \le 0 \tag{35}$$

The preceding constraints are imposed on the skin, stiffener flange, and web laminates, respectively.

Table 1 Table of design variables

	Design variables $\boldsymbol{x}$		
Stiffener type (see Fig. 3)	Skin	Stiffener flange	Stiffener web
a	h $\xi^{A,D}_{[1\ 2\ 3]}$ $t = h$	t_a b_{sf} $\xi^{A,D}_{[1\ 2\ 3]}$ $t_{\text{sf}} = t_a$	h_{sw} $t_{\text{sw}} = 2t_a$
b		As stiffener type a, knowing that $t_{\text{sf}} = t_a$	$t_{\text{sw}} = t_a$
c	h $\xi^{A,D}_{[1\ 2\ 3]}$ $t = h$	t_a b_{sf} $\xi^{A,D}_{[1\ 2\ 3]}$ $t_{\text{sf}} = t_a$	t_w h_{sw} $\xi^{A,D}_{[1\ 2\ 3]}$ $t_{\text{sw}} = 2t_a + t_w$
d		As stiffener type c, knowing that $t_{\text{sf}} = 2t_a$	

4. Strength Constraints

Strength constraints are introduced to limit the magnitude of strains in tension, compression, and shear taken by the laminate; this is conducted in terms of allowable strains. Strains in the x, y, and xy directions are restrained. The strains under the applied in-plane loads are calculated using CLT; hence,

$$\begin{bmatrix} \varepsilon_x^0 \\ \varepsilon_y^0 \\ \varepsilon_{xy}^0 \end{bmatrix} = \begin{bmatrix} A_{11} & A_{12} & A_{16} \\ A_{12} & A_{22} & A_{26} \\ A_{16} & A_{26} & A_{66} \end{bmatrix}^{-1} \begin{bmatrix} N_x \\ N_y \\ N_{xy} \end{bmatrix} \tag{36}$$

A reserve factor or ratio between the allowable and applied strain is defined as

$$RF_i^j = \frac{\varepsilon_{\text{ai}}^j}{\varepsilon_i^{0j}} \qquad i = T, C \qquad j = x, y, xy \tag{37}$$

where T and C denote tension and compression, respectively. The strength constraints for both the tension and compression cases take the following expressions:

$$\frac{1}{RF_i^j} - 1 \leq 0 \qquad i = T, C \qquad j = x, y, xy \tag{38}$$

These constraints are applied to the skin, stiffener flange, and stiffener web laminates, respectively.

5. Buckling Constraints and CF Solutions

Buckling constraints are assessed in terms of local buckling (failure of the skin, the stiffener web, or the local skin-stiffener interaction) and global buckling (failure of the stiffened panel as a whole) criteria. Local and global buckling constraints on anisotropic composite stiffened panels are considered using analytical (CF solutions) and numerical (FE) methods.

This section describes the CF solutions used to assess the local and global buckling behavior of an anisotropic composite stiffened panel; the next section describes the FE analysis.

a. Local Buckling of the Skin. The skin between stiffeners, as shown in Fig. 1, is assumed to be a long flat plate, simply supported along the edges under normal and shear load. Weaver [8,36] recently provided a comprehensive set of CF solutions for long flexural anisotropic plates under compression and shear loading. Note that in addition to presenting a CF solution for the uniaxial compression case, Weaver [8] detailed a procedure to exactly identify the critical uniaxial compression load. Nondimensional parameters were used to calculate buckling coefficients, following Nemeth [7], to obtain the critical buckling load. The nondimensional parameters (e.g., [7]) are defined in terms of the flexural stiffness as follows:

$$\alpha = \sqrt[4]{\frac{D_{22}}{D_{11}}}, \qquad \beta = \frac{D_{12} + 2D_{66}}{\sqrt{D_{11}D_{22}}}, \qquad \gamma = \frac{D_{16}}{\sqrt[4]{D_{11}^3 D_{22}}}$$
$$\delta = \frac{D_{26}}{\sqrt[4]{D_{11}D_{22}^3}} \tag{39}$$

Normal buckling: Weaver [8] approximated the critical buckling load of a long anisotropic plate with simply supported conditions along the edges and under normal loading as follows:

$$N_x^{\text{cr}} = K_x \frac{\pi^2}{b^2} \sqrt{D_{11}D_{22}} \tag{40}$$

where K_x is a nondimensional buckling coefficient given by

$$K_x = 2(1+\beta) - 2(\beta + 3 + 2\gamma^2)\frac{(\gamma + 3\delta)^2}{(\beta+3)^2} - 4(\delta + 2\gamma^3 - \beta\gamma)\frac{(\gamma+3\delta)^3}{(\beta+3)^3} \tag{41}$$

When $|\gamma|$ and $|\delta| < 0.4$, K_x is expected to give sufficient accuracy. For laminates with $|\gamma|$ and $|\delta| > 0.4$, an iteration scheme to calculate K_x is applied (for further details, see [8]). The reserve factor for the uniaxial compression loading is given by

$$RF_{px} = \frac{N_x^{\text{cr}}}{-N_x} \tag{42}$$

Shear buckling: Weaver [36] defined the shear buckling coefficient in terms of the nondimensional parameters as

$$K_{xy} = 3.42 + 2.05\beta - 0.13\beta^2 - 1.79\gamma - 6.89\delta + 0.36\beta(2\gamma + \delta) - 0.25(2\gamma + \delta)^2 \tag{43}$$

The critical shear buckling load has the following expression:

$$N_{xy}^{\text{cr}} = K_{xy} \frac{\pi^2}{b^2} \sqrt[4]{D_{11}D_{22}^3} \tag{44}$$

The reserve factor for the shear buckling is given by

$$RF_{pxy} = \frac{N_{xy}^{\text{cr}}}{|N_{xy}|} \tag{45}$$

In the case of negative shear, the shear buckling coefficient is calculated assuming that each ply angle is reversed in sign. This is the same as changing the sign of the nondimensional parameters δ and γ.

Normal-shear buckling interaction: The following formula [37] is used to address the normal-shear buckling interaction in the skin:

$$\frac{1}{RF_{pb}} = \frac{1}{RF_{px}} + \frac{1}{(RF_{pxy})^2} \tag{46}$$

The constraint for the local buckling of the skin is given by

$$1 - RF_{pb} \leq 0 \tag{47}$$

b. Local Buckling of the Stiffener Web. The stiffener web, as depicted in Fig. 1, is assumed to be a long flat plate, simply supported along three edges (two short edges and one long edge) with one edge free (long edge) under normal load. Weaver and Herencia [38] recently developed a CF solution for this case that includes the effects of flexural anisotropy. The critical buckling load is given by

$$N_{wx}^{\text{cr}} = \frac{12}{b^2}\left(D_{66} - \frac{D_{26}^2}{D_{22}}\right) \tag{48}$$

Note that when there is no flexural anisotropy, the preceding formula reduces to the orthotropic expression [39]. The reserve factor for the stiffener web buckling is given by

$$RF_{\text{wb}} = \frac{N_{wx}^{\text{cr}}}{-N_{wx}} \tag{49}$$

The constraint for the local buckling of the stiffener web is implemented as follows:

$$1 - RF_{\text{wb}} \leq 0 \tag{50}$$

Note that the local buckling of the skin and the stiffener web, are considered separately assuming no interaction between them.

c. Global Longitudinal Buckling. The stiffened panel is assumed to behave as a wide column with pinned ends. The critical buckling load for this case, accounting for the shearing force induced at the stiffener web during buckling [4,40], is given by

$$P_{\text{cr}} = \frac{P_e}{1 + \left(P_e \Big/ A_{\text{sw}} G_{xy}^{\text{sw}}\right)} \tag{51}$$

where

$$P_e = \frac{\pi^2 E I_c}{a^2} \tag{52}$$

The reserve factor for column buckling is calculated by the ratio between the critical column and applied load. Hence,

$$RF_{\text{cb}} = \frac{P_{\text{cr}}}{-F_c} \tag{53}$$

d. Global Shear Buckling. The stiffened panel is assumed to be infinitely long with simply supported conditions along the long edges [4]. The critical shear load is derived from [36], considering that the width of the plate (b) coincides with the length of the stiffened panel (a), and the longitudinal and transversal bending stiffness of the stiffened panel are given, respectively, by

$$D_{11} = D_{22} \tag{54}$$

$$D_{22} = D_c = \frac{EI_c}{b} \tag{55}$$

Substituting the preceding expressions into Eq. (44), the nondimensional parameters can be calculated, and thus a new shear buckling coefficient K_{sh} is found; hence, the critical shear load is as follows:

$$N_{\text{sh}}^{\text{cr}} = K_{\text{sh}} \frac{\pi^2}{a^2} \sqrt[4]{D_c^3 D_{22}} \tag{56}$$

The reserve factor for the overall shear buckling is given by the ratio between the critical and applied shear load; therefore,

$$RF_{\text{sb}} = \frac{N_{\text{sh}}^{\text{cr}}}{|N_{xy}|} \tag{57}$$

As previously stated, in the case of negative shear, the global shear buckling coefficient is calculated assuming that each ply angle is reversed in sign, which is equivalent to changing the sign of the nondimensional parameters δ and γ.

e. Global Longitudinal-Shear Buckling Interaction. An interaction formula [4] is used to address the global buckling constraints. Hence,

$$\frac{1}{RF_{\text{cs}}} = \frac{1}{RF_{\text{cb}}} + \frac{1}{(RF_{\text{sh}})^2} \tag{58}$$

The constraint for the global buckling of the stiffened panel is given by

$$1 - RF_{\text{cs}} \leq 0 \tag{59}$$

6. Buckling Constraints and FE Analysis

MSC/NASTRAN [41] is used to perform linear buckling analysis (SOL 105) [42]. The superstiffener is modeled using quadrilateral elements with four nodes (CQUAD4). A minimum of five nodes are used per half-wavelength [42]. PSHELL and MAT2 cards are used to idealize the skin, stiffener flange, and stiffener web, respectively, for their membrane and bending properties. Rigid body elements (RBE2s) are employed to simulate rigid connections and to account for the offsets between the skin and the stiffener flange and between the stiffener flange and the stiffener web. The superstiffener element is assumed to be simply supported along the short edges and restrained in rotations along the long edges. This rotation provides symmetry conditions and simulates that the stiffened panel consists of a series of superstiffeners. Normal loading is introduced via RBE2 elements, whereas transverse and shear loading are applied by nodal forces. This FE modeling technique captures both local and global buckling behavior of an anisotropic stiffened panel. Figures 5 and 6 show the features of the FE modeling in detail.

7. Practical-Design Constraints

Niu [43] provided a comprehensive summary of design practices for composites. A reduced set of those rules is used as design constraints. For a composite stiffened panel, the design considerations are addressed by limiting the percentages of the 0-, 90-, 45-, and −45- deg ply angles, the skin/stiffener-flange Poisson's ratio mismatch, and the skin gauge. The practical-design constraints are described in the following sections.

a. Percentages of Ply Angles. At least 10% of each ply orientation should be provided [43]. The maximum and minimum percentages of the ply angles for the skin, stiffener flange, and stiffener web are limited. The percentages of the 0-, 90-, 45-, and −45- deg ply angles for each of those elements are

$$p_i = \frac{2t_i}{h} \cdot 100 \qquad i = 0, 90, 45, -45 \qquad h = t, t_{\text{sf}}, t_{\text{sw}} \tag{60}$$

The maximum and minimum allowable ratios are given by

$$RF_{pi}^{\max} = \frac{p_i^{\max}}{p_i} \tag{61}$$

$$RF_{pi}^{\min} = \frac{p_i}{p_i^{\min}} \tag{62}$$

The constraints for the maximum and minimum percentages of the 0-, 90-, 45-, or −45- deg ply angles are as follows:

$$1 - RF_{pi}^{\max} \leq 0 \tag{63}$$

$$\frac{1}{RF_{pi}^{\min}} - 1 \leq 0 \tag{64}$$

b. Skin/Stiffener-Flange Poisson's Ratio Mismatch. The reduction of Poisson's ratio mismatch is critical in composite bonded structures [43]. The difference between the skin and the

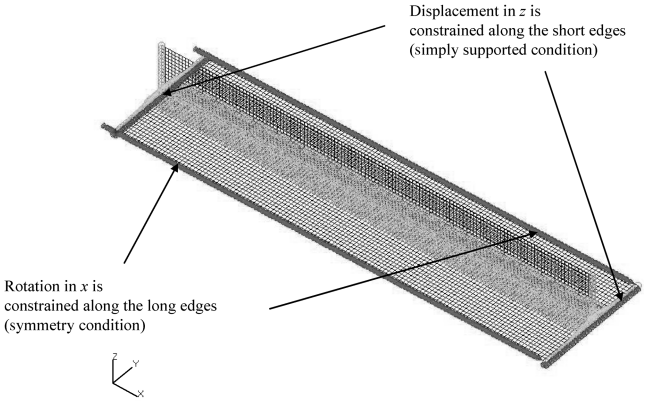

Fig. 5 Superstiffener FE model with boundary conditions.

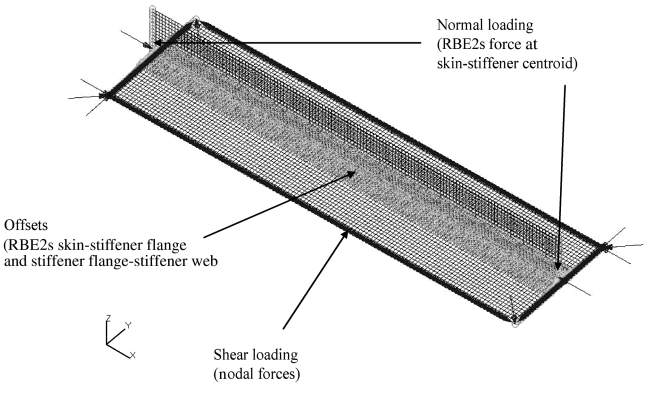

Fig. 6 Superstiffener FE model with combined loading.

stiffener flange Poisson's ratio is limited by a tolerance ζ to reduce the mismatch. An acceptable value of ζ is assumed to be 0.05.

Poisson's ratio-mismatch constraint between the skin and the stiffener flange is given by

$$|\nu_{xy}^{\text{skin}} - \nu_{xy}^{\text{sf}}| - \zeta \leq 0 \tag{65}$$

c. Skin Gauge. The minimum skin gauge is determined by the danger of a puncture due to lightning strike. Niu [43] suggested a minimum skin thickness of 3.81 mm. Skin gauge is addressed by limiting the maximum and minimum skin thickness. The maximum and minimum skin-thickness ratios are given by

$$RF_t^{\max} = \frac{t_{\max}}{t} \tag{66}$$

$$RF_t^{\min} = \frac{t}{t_{\min}} \tag{67}$$

Thus, the skin-gauge constraints are given by

$$1 - RF_t^{\max} \leq 0 \tag{68}$$

$$\frac{1}{RF_t^{\min}} - 1 \leq 0 \tag{69}$$

8. Sensitivities

When FE analysis is used to provide the buckling constraints, sensitivities [44,45] are supplied to MATLAB to decrease the number of FE runs and to accelerate the optimization process. Buckling sensitivities are computed in MSC/NASTRAN using the design sensitivity and optimization solution (SOL 200) [44]. Strength, lamination-parameter, and practical-design constraint sensitivities are calculated by the forward finite difference approximation given by

$$\frac{\partial G_i(\boldsymbol{x})}{\partial x_j} = \frac{G_i(\boldsymbol{x} + \Delta x_j) - G_i(\boldsymbol{x})}{\Delta x_j} \tag{70}$$

where Δx_j is a small perturbation applied to the jth design variable. After a trial-and-error exercise, a suitable step size for the perturbation was determined as 0.0001.

B. Second Step: GA-Based Optimization

A standard GA [20,46] is employed at this step to solve the discrete layup optimization problem. The lamination parameters from the first optimization step are targeted to obtain the laminate stacking sequences for the skin, stiffener flange, and web, respectively. The structure of a standard GA is well reported in the literature [16–20,46]. The structure of the GA herein used consists of the generation of an initial population, evaluation, elitism, crossover, reproduction, and mutation. Note that the GA is applied separately to the skin, stiffener flange, and web.

1. Fitness Function

The fitness function is expressed in terms of the square difference between the optimum and targeted lamination parameters [34]; hence,

$$f(\boldsymbol{y}) = \sum_{i=1}^{3} wf_i^A \left(\xi_i^A - \xi_{\text{iopt}}^A\right)^2 + \sum_{i=1}^{3} wf_i^D \left(\xi_i^D - \xi_{\text{iopt}}^D\right)^2 \tag{71}$$

where $\boldsymbol{y}$ is the design variable vector or gene representing the laminate stacking sequence and $wf_i^{A,D}$ are the lamination-parameter weighting factors. Note that the weighting factors of the lamination parameters were set to unity so that the membrane and bending lamination parameters can have similar effects on the fitness function.

2. Design Constraints

Extra penalty terms are added in Eq. (71) to account for ply-contiguity constraints [13,14,16–18]; thus,

$$g(\boldsymbol{y}) = \sum_{i=1}^{4} \Theta_i \tag{72}$$

where Θ_i is the ith penalty term related to the maximum number of plies of the same orientation that can be stacked together (p). When $p > 4$ (e.g., [13]), the value of Θ_i is one; otherwise, it is zero.

In addition, a stacking-sequence design constraint to locate a set of ± 45- deg plies at the outer surface of the laminate can be enforced during the generation of the initial population.

3. Design Variables: Genes

The design variables are the thicknesses and the 0-, 90-, 45-, or -45- deg ply angles that constitute the laminate stacking sequences for the skin, stiffener flange, and web. Those variables are encoded and modeled as chromosomes in genes within the GA. The corresponding encoded chromosomes to ply angles are 1, 2, 3, 4, 5, 6, and 7 for $\pm 45, 90_2, 0_2, 45, -45, 90$, and 0 deg, respectively. Figure 7 shows the modeling of the gene for the skin. The total skin thickness is given by h, the encoded ply angle is θ, and n corresponds to half- or half-plus-one-plies, depending on whether the skin laminate is symmetric or midplane symmetric.

The modeling of the genes for the stiffener flange and web, respectively, depending on the stiffener type, are given in Fig. 8. The variables t_a and t_w are defined in Table 1, in which ψ and ϕ are the encoded ply angles for the stiffener flange and web, respectively, and m and p are half- or half-plus-one-plies, depending on whether the stiffener flange and web laminates are symmetric or midplane symmetric.

V. Numerical Examples

Reference [18] provides a set of optimum composite panels with blade stiffeners under strength, buckling, and ply-contiguity constraints, in which a GA is employed to carry out the optimization. This work has been used initially to compare this two-step optimization. Note that the set of constraints found in [18] differs slightly from the design constraints described in this paper (especially, the strength constraints). In [18], the failure strength appears to be at ply level, whereas in this paper, it is assessed at laminate level. For comparison purposes, an optimum stiffened panel just under buckling and ply-contiguity constraints is taken from [18]. The superstiffener properties corresponding to the minimum mass design selected are listed in Table 2. Material properties are described in Table 3. The composite stiffened panel is under normal and shear

h	θ_1	θ_2	$\cdots$	$\cdots$	θ_{n-1}	θ_n

$\theta_i = 1,2,3,4,5,6,7$

Fig. 7 Gene with chromosomes for the skin.

Stiffener types a-b

t_a	ψ_1	ψ_2	$\cdots$	$\cdots$	ψ_{m-1}	ψ_m

$\psi_i = 1,2,3,4,5,6,7$

Stiffener types c-d

t_a	ψ_1	ψ_2	$\cdots$	$\cdots$	ψ_{m-1}	ψ_m
t_w	ϕ_1	ϕ_2	$\cdots$	$\cdots$	ϕ_{q-1}	ϕ_q

$\psi_i = \phi_i = 1,2,3,4,5,6,7$

Fig. 8 Genes with chromosomes for the different stiffener types.

loading. The smeared[§] normal and shear loads are −3502.54 and −875.63 N/mm, respectively.

First, the selected design from [18] was assessed, employing the buckling methods described in Secs. IV.A.5 and IV.A.6; results are collected in Table 4. Good agreement in results was found by employing FE. However, CF solutions showed significant discrepancies in results, relative to those reported in [18]. The main reason for these differences lies in the fact that the CF solutions used in this paper do not account for the interaction between the skin and the stiffener. The stiffener will have an impact on the local and global buckling capabilities of the superstiffener element. When a local buckling mode occurs, the skin and stiffener will usually share the same number of longitudinal half-wavelengths. This phenomenon is normally associated with a lower energy state than that resulting from the buckling of the skin or the stiffener web in isolation. In addition, the stiffener flange might act as a reinforcement, locally increasing the stiffness of the skin, and therefore improving its resistance to buckling. Considering the buckling of the skin or the stiffener web in isolation implies that either the skin or the stiffener web presents high stiffness and therefore does not contribute to the local buckling. The CF solutions used herein evaluate the buckling of the skin and the stiffener web in isolation without relating buckling patterns or accounting for the stiffening effect of the stiffener flange in the skin. Consequently, CF solutions predicted lower buckling loads.

Subsequently, the two-step optimization approach was applied. The first-step optimization was set up using stiffener type b, because this is equivalent to the blade stiffener used in [18]. The stiffener flange width was also fixed, because it was not a design variable in [18]. At the second step, a GA code was used with a population of 40, 200 generations, a 0.7 probability of crossover, a 0.05 probability of mutation, and assuming that all weighting factors for the lamination parameters were equal to 1.

Table 5 details the optimum superstiffener designs obtained by this two-step optimization using both FE and CF solutions to assess the buckling constraints. The masses of the continuous M_c and discrete M_d optimizations are provided. The first and fourth optimum designs do not include ply-contiguity constraints. The second, third, and fifth optimum designs include ply-contiguity constraints. Additionally, the third design is further constrained to locate at least one set of ±45- deg plies at the outer surface of the skin and stiffener laminates.

Results show that when employing FE to assess buckling constraints, a lighter design than that in [18] is obtained, even at the expense of adding ply-contiguity constraints. Without ply-contiguity constraints, a 3.5% mass saving is achieved. When ply-contiguity constraints are applied at the second step, the mass savings is 2.7%. It is interesting to see in this case that although ply-contiguity constraints were not included at the first optimization step, they can still be met at the second step with a small mass penalty. From the best optimum solution, it is observed that the skin laminate presents flexural anisotropy and no 0-deg plies. For this specific case, the laminate anisotropy is used to our advantage to improve the buckling load carrying capability of the stiffened panel. In contrast, the stiffener shows a high percentage of 0-deg plies without any 90-deg plies. As one might expect, the skin loses stiffness in the longitudinal direction while improving its buckling resistance. This is compensated with an increase of stiffness in the longitudinal direction in the stiffener to prevent global buckling failure. CF solutions, as expected, offered heavier solutions than those using FE (a maximum of approximately 18.9%) and that reported in [18] (approximately 14.7%). Note that the CF designs were evaluated using FE. The critical buckling load factors are shown in brackets in Table 5.

Table A1 shows the thicknesses and values of the lamination parameters obtained at the first and second optimization steps, respectively, for the skin and the stiffener. It is clearly observed that a good correlation often exists between the lamination parameters at both steps. When ply-contiguity constraints are added, small discrepancies are observed. However, in this case, the optimums still satisfy the design requirements. Note that ply-contiguity constraints will limit the bending lamination parameter ξ_2^D.

Table 2 Superstiffener properties from [18]

M, kg	2.58
a, mm	762
b, mm	203.2
b_{sf}, mm	60.96
h_{sw}, mm	82.55
Layup, skin (32 plies)	$[\pm 45/90_4/(\pm 45)_5]_S$
Layup, stiffener (68 plies)	$[(\pm 45)_4/0_2/(\pm 45)_2/(0_4/\pm 45)_3/0_2]_S$

Table 3 AS4/3502 material properties as in [18]

E_{11}, N/mm^2	127,553.8
E_{22} , N/mm^2	11,307.47
G_{12} , N/mm^2	5998.48
v_{12}	0.3
ρ, kg/mm^3	$1.578\ 10^{-6}$
t_p, mm	0.132

Table 4 Buckling method results

λ_b ([18])	1.0090
λ_b (FE)	1.0299
Closed form	
RF_{px}	0.4869
RF_{pxy}	0.6434
RF_{pb}	0.2238
RF_{wb}	0.7019
RF_{cb}	2.0933
RF_{sh}	5.7728
RF_{cs}	1.9698

Table 5 Optimum superstiffener type-b designs under buckling, with and without ply-contiguity constraints; FE buckling load factors for CF solutions are shown in brackets

Method	M_c/M_d, kg	λ_b/RF_b	h_{sw}, mm	Layup
FE	2.45/2.49	1.0004	74.77	Skin (33 plies) $[90_4/45_3/\pm 45/90/(\pm 45)_3/45]_{MS}$ Stiffener (66 plies) $[(\pm 45)_2/-45/45/(\pm 45_3)/0_8/45/0_{12}]_S$
FE	2.45/2.51	0.9906	74.77	Skin (33 plies) $[(90_2/45)_2/90/45/(\pm 45)_4/45]_{MS}$ Stiffener (67 plies) $[(\pm 45)_2/-45/45/(0_4/\pm 45)_3/0_2/(0_2/90)_2/0/0]_{MS}$
FE	2.45/2.51	0.9940	74.77	Skin (33 plies) $[\pm 45/90_4/45/90_2/45_2/(\pm 45)_2/45/-45]_{MS}$ Stiffener (67 plies) $[(\pm 45)_3/0_2/45/(0_2/\pm 45)_2/0_4/45/(0_4/-45)_2/0/0]_{MS}$
CF	2.94/2.96	0.9972 (1.3281)	75	Skin (45 plies) $[(\pm 45)_2/45_3/(90_2/45)_2/90_4/45/90_4/45]_{MS}$ Stiffener (70 plies) $[(\pm 45)_7/0_2/(\pm 45)_2/0_{15}]_S$
CF	2.94/2.96	0.9862 (1.3203)	75	Skin (45 plies) $[(\pm 45)_2/45_4/(90_4/45)_2/90_4/45]_{MS}$ Stiffener (71 plies) $[(\pm 45)_6/0_2/\pm 45/0_4/\pm 45/0_2/90/0_4/-45/0_4/45/-45]_{MS}$

[§]Shared by the skin and stiffener.

Table 6 Optimum superstiffener type-b designs under buckling, practical-design, and ply-contiguity constraints; FE buckling load factors for CF solutions are shown in brackets

Practical design	Method	M_c/M_d, kg	λ_b/RF_b	h_{sw}, mm	Layup
10%	FE	2.51/2.54	0.9967	74.97	Skin (38 plies) $[\pm 45/90_4/45_2/90/45_2/0/\pm 45/45/0_2/\pm 45]_S$ Stiffener (61 plies) $[45/(\pm 45)_4/-45/0_4/\pm 45/0_4/90_2/0_3/90/0_4/90]_{MS}$
	CF	2.97/3.01	0.9837 (0.8904)	75	Skin (62 plies) $[(\pm 45)_6/0_2/\pm 45/(0_4/90_2)_2/90/0_2]_S$ Stiffener (47 plies) $[(\pm 45)_4/-45/(\pm 45)_4/90_2/0_3/90/0]_{MS}$
Poisson's ratio mismatch	FE	2.50/2.54	1.0011	74.67	Skin (38 plies) $[\pm 45/90_2/45_4/90/\pm 45/0_2/(\pm 45)_2/0/0]_S$ Stiffener (61 plies) $[(\pm 45)_3/-45/\pm 45/0_4/\pm 45/0_3/90/0_4/-45/0_4/90/0/0]_{MS}$
	CF	2.94/2.98	0.9907 (1.2434)	75	Skin (47 plies) $[\pm 45/45/(\pm 45)_3/-45_2/(45/-45_4)_2/\pm 45/-45]_{MS}$ Stiffener (68 plies) $[(\pm 45)_8/(0_4/\pm 45)_2/0_4/45/0]_S$

Furthermore, the effect of practical-design constraints on the optimum design was assessed. Table 6 gives the optimum superstiffener designs obtained for stiffener type b when buckling; practical-design constraints (such as at least 10% of each ply orientation or skin/stiffener-flange Poisson's ratio mismatch) and ply contiguity, as well as at least one set of ±45- deg plies at the outer surfaces of the skin and stiffener laminates, are included in the optimization.

Results show a mass penalty (a maximum of 2% when FE is used, in comparison with the first design in Table 5) when practical-design constraints are applied. Those practical constraints reduce the size of the membrane and bending lamination-parameter design space. For example, when the 10% rule is applied, the new feasible membrane lamination design space changes from Eq. (20) to the following expressions:

$$2|\xi_1^A| - \xi_2^A - 0.6 \leq 0 \tag{73}$$

$$\xi_2^A - 0.8 \leq 0 \tag{74}$$

As previously stated, differences between FE and CF solutions were found. The practical-design constraint of minimum skin gauge was not considered because, in this case, it had no effect on the optimum design. Table A2 gives the thicknesses and values of the lamination parameters obtained at the first and second optimization steps. The CF designs were also checked using FE. Their critical buckling load factors are shown in brackets in Table 6. Note that the CF optimum design when the 10% rule is applied has a buckling load factor less than unity. In this case, CF solutions predict that the local and global failure modes are very close. This suggests that the FE technique used herein might provide conservative results if the global buckling failure is close to the driving mode of failure.

Finally, the effect of the stiffener type on the optimum design under strength, buckling, and practical-design constraints was evaluated. For this case, at the first step, the stiffener flange width was freed and considered as a design variable. Common aerospace design strain levels of 3600 microstrains ($\mu\varepsilon$) in both tension and compression and 7200 $\mu\varepsilon$ in shear were imposed. Stacking-sequence constraints such as ply contiguity and at least one set of ±45- deg plies at the outer surface of the skin and stiffener laminates were added at the second step. Table 7 provides the optimum superstiffener designs obtained under those constraints.

Under these circumstances, the optimum design obtained by the FE and CF solutions did not differ so significantly (a maximum of approximately 8.4%). This is because strength is the driven constraint. The stiffener type seems to have an impact on the design (maximums of approximately 3.9 and 7.3% when using FE and CF solutions, respectively). Note that the optimum continuous designs obtained with FE do not practically vary, in contrast to those using CF solutions (a maximum of approximately 7.6%). Note also that in

Table 7 Optimum superstiffener designs under buckling, strength, practical-design, and ply-contiguity constraints; FE buckling load factors for CF solutions are shown in brackets

Stiffener type	Method	M_c/M_d, kg	λ_b/RF_b	λ_s/RF_s	b_{sf}, mm	h_{sw}, mm	Layup
a	FE	2.74/2.89	1.0761	0.9952	60.01	69.95	Skin (59 plies) $[\pm 45/45_3/90_2/(\pm 45/0_4)_2/45/0_4/45/0_2/90/0/0]_{MS}$ Stiffener flange (31 plies) $[\pm 45/90/-45/0_4/45/0_4/90/0/0]_{MS}$
	CF	2.93/3.05	1.0272 (1.0971)	0.9827	60	70	Skin (65 plies) $[(\pm 45)_2/0/(\pm 45)_2/0_4/45/0_2/90/0_2/45/(0_4/90)_2/90/0/0]_{MS}$ Stiffener flange (30 plies) $[(\pm 45)_3/-45/0_3/(90/0)_2/0]_S$
b	FE	2.74/2.84	1.0660	1.0034	60.01	69.96	Skin (58 plies) $[\pm 45/90_2/45/\pm 45/0_2/45_2/(45/0_4)_2/90/0_4/-45/0_2]_S$ Stiffener (47 plies) $[(\pm 45)_2/0_2/90_2/0_4/-45/0_4/90/0_4/45/0]_{MS}$
	CF	2.99/3.08	1.0020 (0.9805)	0.9827	60	70.03	Skin (66 plies) $[(\pm 45)_2/0/\pm 45/90/(0_4/45)_2/90_2/0_4/\pm 45/0_4/90/0_2]_S$ Stiffener (46 plies) $[\pm 45/45/(\pm 45)_2/-45/\pm 45/0_2/\pm 45/90/0_2/90_2/0_3/90]_S$
c	FE	2.73/2.89	1.0888	0.9906	59.99	69.67	Skin (61 plies) $[\pm 45/45/90_2/45/(\pm 45/0_2)_2/0_2/45/0_3/45/0_2/90/0_4/-45/0/0]_{MS}$ Stiffener flange (18 plies) $[\pm 45/0_2/45/0/-45/90/0]_S$ Web (32 plies) $[0_2/90/0_2/-45/0_2/45/0_4/90/0_2]_S$
	CF	2.79/2.87	1.0081 (1.0228)	0.9920	60	70	Skin (65 plies) $[\pm 45/45/(\pm 45)_2/0_3/90_2/0_2/45/0_2/-45/0_4/90/0_4/45/0_4/90]_{MS}$ Stiffener flange (9 plies) $[\pm 45/45/90/0]_{MS}$ Web (44 plies) $[-45_2/0/-45/0_2/-45/0_4/-45/0_2/90/0_4/90/0_2]_S$
d	FE	2.73/2.95	1.0948	1.0350	59.76	69.69	Skin (63 plies) $[\pm 45/45/\pm 45/0_2/90/\pm 45/45/0_4/90/(90/0_4)_2/45/0_4/-45]_{MS}$ Stiffener flange (8 plies) $[\pm 45/90/0]_S$ Web (53 plies) $[0_4/\pm 45/0_2/-45/0_4/45/(0_4/90)_2/90/0/0]_{MS}$
	CF	2.78/3.02	1.0204 (1.1177)	0.9920	60	70	Skin (65 plies) $[(\pm 45)_3/0_2/90_3/(0_2/45)_2/0_4/-45/0_3/45/0_4/90/0/0]_{MS}$ Stiffener flange (8 plies)$[\pm 45/90/0]_S$ Web (53 plies) $[(\pm 45)_4/0_2/-45/90_2/0_4/-45/0_4/90/0/-45/0/0]_{MS}$

the cases of stiffener types c and d, the stiffener-flange minimum thickness was considered to be at least four plies. It was observed that for these two stiffener types, the thickness of flanges tended to a minimum, which suggests that in this case, no flanges might be needed. However, if T-shaped stiffeners are used, the flanges have to provide a certain degree of integrity to the joint with the skin. The thicknesses and values of the lamination parameters for both the first and second optimization steps associated with the results shown in Table 7 are listed in Table A3. Adequate to good agreement is found in all cases. CF designs were also evaluated using FE. The critical buckling load factors are shown in brackets in Table 7.

VI. Conclusions

A method to optimize long anisotropic laminated fiber composite panels with T-shaped stiffeners was developed. The optimization problem was divided into two steps. At the first step, a single superstiffener representing the stiffened panel was optimized using MP techniques and lamination parameters accounting for their membrane and flexural anisotropy. The superstiffener was subjected to a combined loading under strength, buckling, stiffener manufacturability, and practical-design constraints. The skin and stiffener laminates were assumed to be symmetric or midplane symmetric laminates with 0-, 90-, 45-, or −45- deg ply angles. The dimensions and values of the lamination parameters for an optimum superstiffener design were obtained. At the second step, a GA code was used to target the optimum lamination parameters to find the actual layups for the superstiffener laminates (skin, stiffener flange, and stiffener web), considering ply contiguity and the stiffener manufacture, without performing structural analysis.

This two-step approach showed good performance when compared with other work ([18]). Optimized panels obtained here under buckling and ply-contiguity constraints were approximately 2.7% lighter than those optimized and reported in [18]. A direct comparison with the optimized results of [18] was difficult because this paper used a representative skin-stiffener element (superstiffener) with continuity conditions (so as to increase computational efficiency) to model the stiffened panel, whereas that reported in [18] was a stiffened panel made of four stiffeners with simply supported edges. To assess the viability of such an approach, a four-stiffener panel was also studied that reflected the material, layup, and geometry of the optimized panel in [18]. This model gave a buckling-load factor that was approximately 4% greater than that using a single superstiffener. This result showed the built-in conservatism of the continuity constraints for the single superstiffener and presumably related, in part, to the longer wavelength in the buckling mode that was manifested; as such, mass savings reported herein are conservative.

The inclusion of membrane and flexural anisotropy in the optimization procedure enabled more designs to be explored. Thus, elastic tailoring was used to an advantage. Employing FE to assess buckling behavior highlighted the importance of considering the skin-stiffener interaction. CF solutions did not consider this interaction and the resulting structures were heavier. However, CF solutions provide the designer with a valuable understanding of the buckling phenomena.

When considering practical-design constraints, slight mass penalties were observed. If the design is driven by strength constraints, the use of FE or CF solutions to evaluate buckling response showed that results did not differ as much as when buckling was the critical constraint. Stiffener manufacture did seem to have an impact on mass, especially when CF solutions were employed (a maximum of approximately 7.3%); however, it might more substantially affect the design when buckling is the driving constraint.

In general, good agreement was found between the lamination parameters obtained at the first step and those determined from the second step (where the actual stacking sequence is identified). Note that although sometimes the lamination parameters at both steps did not completely match, good designs were still produced. It is also clear that the designs at the first step will always be lighter than the second-step designs, because at the latter step, a rounding process occurs.

The computational cost associated with both gradient and GA optimization was acceptable in this study. Furthermore, it is hoped that this two-step optimization approach will be a module within a more general optimization procedure that could perform elastic tailoring in more complex structures.

Appendix A: Optimum Thicknesses and Lamination Parameters

This Appendix contains the tables with the thicknesses and values of the lamination parameters at the two optimization steps for the optimum designs presented.

Table A1 Optimum/actual thicknesses and lamination parameters under buckling, with and without ply-contiguity constraints

				Membrane lamination parameters			Bending lamination parameters		
			h, mm	ξ_1^A	ξ_2^A	ξ_3^A	ξ_1^D	ξ_2^D	ξ_3^D
Skin	FE	First step	4.2574	−0.2710	−0.4581	0.1922	−0.6126	0.2251	0.3042
		Second step	4.3560	−0.3030	−0.3939	0.2121	−0.5980	0.1960	0.2693
Stiffener		First step	8.6626	0.6248	0.2555	0.0179	0.2413	−0.5000	0.0268
		Second step	8.7120	0.6061	0.2121	0.0303	0.2447	−0.5107	0.0307
Skin	FE	First step	4.2574	−0.2710	−0.4581	0.1922	−0.6126	0.2251	0.3042
		Second step	4.3560	−0.3030	−0.3939	0.2121	−0.5973	0.1946	0.2900
Stiffener		1st step	8.6626	0.6248	0.2555	0.0179	0.2413	−0.5000	0.0268
		Second step	8.8440	0.5224	0.2836	0.0000	0.4065	−0.1776	0.0134
Skin	FE	First step	4.2574	−0.2710	−0.4581	0.1922	−0.6126	0.2251	0.3042
		Second step	4.3560	−0.3636	−0.2727	0.2121	−0.5179	0.0358	0.1545
Stiffener		First step	8.6626	0.6248	0.2555	0.0179	0.2413	−0.5000	0.0268
		Second step	8.8440	0.5821	0.1642	0.0000	0.3648	−0.2704	0.0780
Skin	CF	First step	5.9234	−0.5681	0.1363	0.2838	−0.1834	−0.6332	0.4046
		Second step	5.9400	−0.5333	0.0667	0.2889	−0.2494	−0.5012	0.3280
Stiffener		First step	9.1306	0.4652	−0.0695	0.0000	0.1007	−0.7986	0.0000
		Second step	9.2400	0.4857	−0.0286	0.0000	0.1347	−0.7305	0.0322
Skin	CF	First step	5.9234	−0.5681	0.1363	0.2838	−0.1834	−0.6332	0.4046
		Second step	5.9400	−0.5333	0.0667	0.2889	−0.2347	−0.5307	0.3428
Stiffener		First step	9.1306	0.4652	−0.0695	0.0000	0.1007	−0.7986	0.0000
		Second step	9.3720	0.4225	−0.0423	−0.0141	0.1867	−0.5941	0.0261

Table A2 Optimum/actual thicknesses and lamination parameters under buckling, practical-design, and ply-contiguity constraints

				Membrane lamination parameters			Bending lamination parameters		
			h, mm	ξ_1^A	ξ_2^A	ξ_3^A	ξ_1^D	ξ_2^D	ξ_3^D
Skin	FE	First step	4.9039	−0.0252	−0.2293	0.2103	−0.4878	0.0165	0.3393
		Second step	5.0160	−0.1053	−0.1579	0.2632	−0.4114	−0.0459	0.2282
Stiffener		First step	8.0145	0.4258	0.2516	0.0154	0.0540	−0.5000	0.0120
		Second step	8.0520	0.3770	0.2131	0.0000	0.2091	−0.4945	0.0734
Skin	CF	First step	8.1473	0.3120	0.0239	0.0001	0.0056	−0.7316	0.0781
		Second step	8.1840	0.2258	0.0968	0.0000	0.1303	−0.6428	0.0334
Stiffener		First step	5.9670	0.0734	−0.4532	−0.0001	0.0184	−0.9591	0.0000
		Second step	6.2040	0.0213	−0.4468	−0.0426	−0.0076	−0.9577	0.0034
Skin	FE	First step	4.9546	0.1316	−0.2708	0.1559	−0.2951	−0.3487	0.4727
		Second step	5.0160	0.0526	−0.2632	0.2105	−0.2282	−0.3664	0.3286
Stiffener		First step	7.9078	0.5621	0.2599	0.0217	0.2466	−0.5000	−0.0003
		Second step	8.0520	0.4754	0.2131	−0.0656	0.2561	−0.4251	−0.0404
Skin	CF	First step	6.0678	−0.0002	−0.9996	−0.3976	−0.0006	−0.9989	0.3172
		Second step	6.2040	0.0000	−1.0000	−0.3191	0.0000	−1.0000	−0.0071
Stiffener		First step	8.9045	0.3999	−0.2001	0.0000	0.0640	−0.8721	0.0000
		Second step	8.9760	0.3824	−0.2353	0.0294	0.1148	−0.7704	0.0350

Table A3 Optimum/actual thicknesses and lamination parameters for different stiffener types under buckling, strength, practical-design, and ply-continuity constraints

					Membrane lamination parameters			Bending lamination parameters		
	Stiffener type			h, mm	ξ_1^A	ξ_2^A	ξ_3^A	ξ_1^D	ξ_2^D	ξ_3^D
a	Skin	FE	First step	7.6307	0.4603	0.3206	0.1208	−0.0028	−0.2908	0.3911
			Second step	7.7880	0.4237	0.2542	0.1695	0.1346	−0.2123	0.2672
	Stiffener flange		First step	3.6428	0.5862	0.5724	0.0002	0.1603	−0.0281	0.0016
			Second step	4.0920	0.4839	0.4839	0.0000	0.2261	0.0102	−0.0532
	Skin	CF	First step	8.3976	0.5111	0.4221	0.0889	0.0968	−0.2810	0.0985
			Second step	8.5800	0.4462	0.3846	0.0615	0.3420	−0.1995	0.0659
	Stiffener flange		First step	3.6517	0.2543	0.0441	0.0000	0.0949	−0.7154	0.0000
			Second step	3.9600	0.2667	0.0667	−0.0667	0.1043	−0.6966	−0.0003
b	Skin	FE	First step	7.5512	0.4551	0.3102	0.1449	0.0434	−0.1356	0.2124
			Second step	7.6560	0.4483	0.3103	0.1379	0.1098	−0.0872	0.2314
	Stiffener		First step	5.7497	0.5934	0.5868	0.0009	0.1674	−0.0011	0.0036
			Second step	6.2040	0.4894	0.4894	0.0000	0.2744	0.0862	−0.0079
	Skin	CF	First step	8.3976	0.5111	0.4221	0.0889	0.0968	−0.2810	0.0985
			Second step	8.7120	0.4545	0.3939	0.0606	0.3158	−0.0180	0.0623
	Stiffener		First step	5.9983	0.2033	−0.0175	0.0000	0.1105	−0.7629	0.0000
			Second step	6.0720	0.1304	−0.0435	0.0000	0.0703	−0.7378	0.0848
c	Skin	FE	First step	8.0150	0.4850	0.3700	0.0866	−0.0185	−0.1623	0.2797
			Second step	8.0520	0.4426	0.2787	0.0984	0.1303	−0.1244	0.1853
	Stiffener flange		First step	1.8433	0.3941	0.1881	0.0000	0.3239	−0.2744	0.1030
			Second step	2.3760	0.3333	0.1111	0.0000	0.3416	−0.2785	0.1235
	Web		First step	3.9359	0.7541	0.9083	−0.0198	0.6044	0.7372	−0.0542
			Second step	4.2240	0.6250	0.7500	0.0000	0.6016	0.7559	−0.0396
	Skin	CF	First step	8.3976	0.5111	0.4221	0.0889	0.0968	−0.2810	0.0985
			Second step	8.5800	0.4769	0.3846	0.0615	0.2536	−0.1343	0.1046
	Stiffener flange		First step	1.0560	−0.0182	−0.4414	0.3818	0.0762	−0.8269	0.0594
			Second step	1.1880	−0.1111	−0.3333	0.2222	−0.0343	−0.9259	0.3649
	Web		First step	5.7738	0.6268	0.5823	−0.1901	0.4668	−0.0095	−0.4692
			Second step	5.8080	0.5909	0.5455	−0.2273	0.5208	0.1121	−0.4439
d	Skin	FE	First step	8.0810	0.4887	0.3775	0.0796	0.0217	−0.2271	0.2897
			Second step	8.3160	0.4444	0.3968	0.0794	0.2312	−0.0932	0.1409
	Stiffener flange		First step	0.5280	−0.0277	−0.3359	0.0000	0.2961	−0.0299	0.0473
			Second step	1.0560	0.0000	0.0000	0.0000	−0.0937	−0.7500	0.2813
	Web		First step	6.9947	0.6947	0.7412	0.0000	0.6671	0.3370	0.0321
			Second step	6.9960	0.6226	0.6981	0.0000	0.7464	0.5427	−0.0181
	Skin	CF	First step	8.3976	0.5111	0.4221	0.0889	0.0968	−0.2810	0.0985
			Second step	8.5800	0.4462	0.3846	0.0615	0.1948	−0.0534	0.0631
	Stiffener flange		First step	0.5280	0.3758	0.1516	0.2150	0.3645	−0.2670	0.0745
			Second step	1.0560	0.0000	0.0000	0.0000	−0.0937	−0.7500	0.2813
	Web		First step	6.7055	0.4333	0.2665	−0.0352	0.1538	−0.4921	−0.1131
			Second step	6.9960	0.3585	0.1698	−0.1132	0.1442	−0.4296	−0.0260

Acknowledgments

The authors thank the European Commission (EC) for the Marie Curie Excellence grant MEXT-CT-2003-002690. The first and second authors thank Cezar Diaconu for his contribution and support, particularly on lamination parameters. The first author wishes to thank Tim Edwards and Yoann Bonnefon for their interest, help, and valuable comments, especially on the finite element (FE) method, as well as Mike Coleman and Andrew Main for their assistance on the creation of FE models. Furthermore, the first author thanks Mark Lillico for his comments on the modeling of stiffened panels, as well as Imran Khawaja, Alastair Tucker, Stuart King, Pedro Raposo, and Paul Harper for their general remarks.

References

[1] Jones, R. M., "Mechanics of Composite Materials," 2nd ed., Taylor and Francis, Philadelphia, 1999.

[2] Schmit, L. A., and Farshi, B., "Optimum Laminate Design for Strength and Stiffness," *International Journal for Numerical Methods in Engineering*, Vol. 7, No. 4, 1973, pp. 519–536.

[3] Schmit, L. A., and Farshi, B., "Optimum Design of Laminated Fiber Composite Plates," *International Journal for Numerical Methods in Engineering*, Vol. 11, No. 4, 1977, pp. 623–640.

[4] Stroud, W. J., and Agranoff, N., "Minimum Mass Design of Filamentary Composite Panels Under Combined Loads: Design Procedure Based on Simplified Equations," NASA TN D-8257, 1976.

[5] Ashton, J. E., and Waddoups, M. E., "Analysis of Anisotropic Plates," *Journal of Composite Materials*, Vol. 3, No. 1, 1969, pp. 148–165.

[6] Chamis, C. C., "Buckling of Anisotropic Composite Plates," *Journal of the Structural Division*, Vol. 95, No. ST10, 1969, pp. 2119–2139.

[7] Nemeth, M. P., "Importance of Anisotropy on Buckling of Compression-Loaded Symmetric Composite Plates," *AIAA Journal*, Vol. 24, No. 11, 1986, pp. 1831–1835.

[8] Weaver, P. M., "Approximate Analysis for Buckling of Compression Loaded Long Rectangular Plates with Flexural/Twist Anisotropy," *Philosophical Transactions of the Royal Society of London, Series A: Mathematical and Physical Sciences*, Vol. 462, No. 2065, 2006, pp. 59–74.

[9] Tsai, S. W., Halpin, J. C., and Pagano, N. J., *Composite Materials Workshop*, Technomic, Stamford, CT, 1968, pp. 233–253.

[10] Tsai, S. W., and Hahn, H. T., *Introduction to Composite Materials*, Technomic, Stamford, CT, 1980.

[11] Miki, M., and Sugiyama, Y., "Optimum Design of Laminated Composite Plates Using Lamination Parameters," AIAA Paper 1991-971, 1991.

[12] Fukunaga, H., and Vanderplaats, G. N., "Stiffness Optimization of Orthotropic Laminated Composites Using Lamination Parameters," *AIAA Journal*, Vol. 29, No. 4, 1991, pp. 641–646.

[13] Haftka, R. T., and Walsh, J. L., "Stacking Sequence Optimization for Buckling of Laminated Plates by Integer Programming," *AIAA Journal*, Vol. 30, No. 3, 1992, pp. 814–819.

[14] Nagendra, S., Haftka, R. T., and Gürdal, Z., "Stacking Sequence Optimization of Simple Supported Laminates with Stability And Strain Constraints," *AIAA Journal*, Vol. 30, No. 8, 1992, pp. 2132–2137.

[15] Fukunaga, H., Sekine, H., Sato, M., and Iino, A., "Buckling Design of Symmetrically Laminated Plates Using Lamination Parameters," *Computers and Structures*, Vol. 57, No. 4, 1995, pp. 643–649.

[16] Le Riche, R., and Haftka, R. T., "Optimization of Laminate Stacking Sequence for Buckling Load Maximization by Genetic Algorithm," *AIAA Journal*, Vol. 31, No. 5, 1993, pp. 951–956.

[17] Nagendra, S., Haftka, R. T., and Gürdal, Z., "Design of a Blade Stiffened Composite Panel by Genetic Algorithm," AIAA Paper 1993-1584, 1993.

[18] Nagendra, S., Jestin, D., Gürdal, Z., Haftka, R. T., and Watson, L. T., "Improved Genetic Algorithm for the Design of Stiffened Composite Panels" *Computers and Structures*, Vol. 58, No. 3, 1996, pp. 543–555.

[19] Goldberg, D. E., *Genetic Algorithms in Search, Optimization and Machine Learning*, Addison Wesley Longman, Reading, MA, 1989.

[20] Coley, D. A., *An Introduction to Genetic Algorithms for Scientist and Engineers*, World Scientific, Singapore, 1999.

[21] Wittrick, W. H., and Williams, F. W., "Buckling and Vibration of Anisotropic or Isotropic Plate Assemblies Under Combined Loadings," *International Journal of Mechanical Sciences*, Vol. 16, No. 4, 1974, pp. 209–239.

[22] Stroud, W. J., and Anderson, M. S., "PASCO-Structural Panel Analysis and Sizing Code, Capability and Analytical Foundations," NASA TM-80181, 1981.

[23] Vanderplaats, G. N., "A Fortran Program for Constrained Function Minimization: User's Manual," NASA TM-X-62282, 1973.

[24] Bushnell, D., "PANDA2-Program for Minimum Weight Design of Stiffened, Composite, Locally Buckled Panels," *Computers and Structures*, Vol. 25, No. 4, 1987, pp. 469–605.

[25] Bushnell, D., "Theoretical Basis of the Panda Computer Program for Preliminary Design of Stiffened Panels Under Combined In-Plane Loads," *Computers and Structures*, Vol. 27, No. 4, 1987, pp. 541–563.

[26] Almoroth, B. O., and Brogan, F. A., "The STAGS Computer Code," NASA CR-2950, 1976.

[27] Liu, W., Butler, R., Mileham, A. R., and Green, A. J., "Bi-Level Optimization and Postbuckling of Highly Strained Composite Stiffened Panels," *AIAA Journal*, Vol. 44, No. 11, 2006, pp. 2562–2570.

[28] Butler, R., and Williams, F. W., "Optimum Design Features of VICONOPT, an Exact Buckling Program for Prismatic Assemblies of Anisotropic Plates," AIAA Paper 1990-1068, 1990.

[29] Yamazaki, K., "Two-Level Optimization Technique of Composite Laminate Panels by Genetic Algorithms," AIAA Paper 1996-1539, 1996.

[30] Autio, M., "Determining the Real Lay-Up of a Laminate Corresponding to Optimal Lamination Parameters by Genetic Search," *Structural and Multidisciplinary Optimization*, Vol. 20, No. 4, 2000, pp. 301–310.

[31] Todoroki, A., and Haftka, R. T., "Lamination Parameters for Efficient Genetic Optimization of the Stacking Sequences of Composite Panels," AIAA Paper 98-4816, 1998.

[32] Liu, B., Haftka, R. T., and Trompette, P., "Maximization of Buckling Loads of Composite Panels Using Flexural Lamination Parameters," *Structural and Multidisciplinary Optimization*, Vol. 26, Nos. 1–2, 2004, pp. 28–36.

[33] Liu, B., and Haftka R. T., "Single Level Composite Wing Optimization Based on Flexural Lamination Parameters," *Structural and Multidisciplinary Optimization*, Vol. 26, Nos. 1–2, 2004, pp. 111–120.

[34] Diaconu, C. G., and Sekine, H., "Layup Optimization for Buckling of Laminated Composite Shells with Restricted Layer Angles," *AIAA Journal*, Vol. 42, No. 10, 2004, pp. 2153–2163.

[35] MATLAB, Software Package, Ver. 7.1, The MathWorks, Inc., Natick, MA, 1994–2006.

[36] Weaver, P. M., "On Optimization of Long Anisotropic Flat Plates Subject to Shear Buckling Loads," 45th AIAA/ASME/ASCE/AHS/ACS Structures, Structural Dynamics and Materials Conference, Palm Springs, CA, AIAA Paper 2004-2053, 2004.

[37] Lekhnitskii, S. G., *Anisotropic Plates*, Gordon and Breach, New York, 1968.

[38] Weaver, P. M., and Herencia, J. E., "Buckling of a Flexurally Anisotropic Plate with One Edge Free," 48th AIAA/ASME/ASCE/AHS/ACS Structures, Structural Dynamics and Materials Conference, Honolulu, HI, AIAA Paper 2007-2413, 2007.

[39] Kollár, L. P., and Springer, G. S., *Mechanics of Composite Structures*, Cambridge Univ. Press, New York, 2003.

[40] Timoshenko, S. P., and Gere, J. M., *Theory of Elastic Stability*, 2nd ed., McGraw–Hill, New York, 1961.

[41] MSC/NASTRAN, Software Package, Ver. 2005, MSC.Software Corp., Santa Ana, CA, 2005.

[42] Lee, J. M. (ed.), *MSC/NASTRAN Linear Static Analysis User's Guide*, MSC.Software Corp., Santa Ana, CA, 2003, Chap. 13.

[43] Niu, C. Y. M., *Composite Airframe Structures: Practical Design Information and Data*, Conmilit, Hong Kong, 1992.

[44] Johnson, E. H., *MSC/NASTRAN Design Sensitivity and Optimization User's Guide*, MSC.Software Corp., Santa Ana, CA, 2004.

[45] Vanderplaats, G. N., *Numerical Optimization Techniques for Engineering Design*, 3rd ed., Vanderplaats Research & Development, Inc., Colorado Springs, CO, 2001.

[46] Gürdal, Z., Haftka, R. T., and Hajela, P., *Design Optimization of Laminated Composite Materials*, Wiley, New York, 1999.

A. Roy
Associate Editor